Deformation Mechanisms and Fracture Toughness of Polystyrene/High-Density Polyethylene Blends Compatibilized by Triblock Copolymer

S. A. XU,* S. C. TJONG

Department of Physics and Materials Science, City University of Hong Kong, 83 Tat Chee Avenue, Kowloon, Hong Kong

Received 29 April 1999; accepted 3 June 1999

ABSTRACT: A dilatometric technique was used to explore the tensile deformation mechanisms of polystyrene (PS)/high-density polyethylene (HDPE) blends compatibilized by a styrene–ethylene–butylene–styrene (SEBS) triblock copolymer. The volume change of the sample during a uniaxial tensile process was determined with two extensometers, and it provided useful information concerning the tensile deformation mechanism. A simple model was used in this study in order to obtain quantitative information on the separate contributions of several possible deformation modes to the total deformation. The results indicated that elastic deformation was the main deformation mode for PS. However, elastic deformation was the main mode of deformation prior to yielding for SEBS compatibilized PS/HDPE blends; thereafter the plastic deformations (including shear and crazing) appeared to dominate over the elastic deformation. Moreover, crazing was the main plastic deformation mode for the blend containing 20 wt % HDPE, and shear deformation became predominant when the HDPE content was further increased. Finally, the essential work concept was used to determine the fracture toughness of the typical ductile PS/HDPE/SEBS 10/80/10 blends. © 2000 John Wiley & Sons, Inc. J Appl Polym Sci 77: 2024–2033, 2000

Key words: dilatometry; deformation mechanism; polystyrene; polyethylene; fracture toughness; essential work

INTRODUCTION

Glassy polymers form a large class of industrially important materials, but the poor ductility and toughness of these polymers has limited their application in engineering sectors.[1–3] Polystyrene (PS) is generally characterized as a hard, transparent, and brittle polymer. Polymer scientists have expended much effort to improve the toughness of PS over the past few decades. A family of polymer blends such as high-impact PS (HIPS) and acrylonitrile–butadiene–styrene copolymer has been developed via the incorporation of elastomeric particles into PS. The addition of a low-modulus rubbery component generally leads to a sharp decrease in the tensile modulus and strength of the blends. Therefore, several workers have attempted to improve the mechanical performance of PS by blending it with ductile thermoplastics that have a higher modulus than rubber, for example, polyolefins (high-density polyethylene, HDPE).[3–9] The morphology, compatibility, and mechanical properties of PS/HDPE blends are well documented.[3,8,9] However, little information is available on the toughening deformation mechanism of a PS/HDPE system.

**Present address:* Institute of Polymer Engineering and Science, East China University of Science and Technology, 130 Mei Long Road, Shanghai 200237, China.

Correspondence to: S. C. Tjong.

Journal of Applied Polymer Science, Vol. 77, 2024–2033 (2000)

In general, the volume change of a polymer specimen during the tensile process can be used to reveal microscopic mechanisms. The shear deformation generally produces no volume change whereas the crazing–cavitation deformation results in a dramatic increase in the volume strain. A number of studies on the deformation mechanisms of unfilled and reinforced polymers are reported in the literature.[10–27] For example, Bucknall and Clayton[28,29] used this method to analyze the creep data and to study the deformation process of rubber toughened plastics. Similarly, Heikens and coworkers[10–16] used this concept to determine the volume strain of a specimen during tensile deformation by simultaneously measuring the axial and transverse strain. Schwarz et al. carried out a preliminary study on the dilatometric behavior of HDPE/polyether copolymer (PEC)/PS blends containing various amounts of styrene–ethylene–butylene–styrene (SEBS). In this system, HDPE formed one phase while the other phase contained either PS or miscible PEC/PS mixtures. They indicated that PS/PEC blends underwent a craze to shear yielding transition at between 40 and 60% PS. However, such a transition occurred at higher PS concentrations when SEBS was added.[27]

In a previous article[3] we studied the tensile and impact properties of HDPE/PS blends compatibilized with an SEBS triblock copolymer. Tensile measurements showed that the elongation at break of HDPE/PS blends tended to increase dramatically with increasing HDPE content. Charpy impact measurements indicated that the impact strength of the blends increased slowly with HDPE content up to 50 wt %, followed by a significant increase with further increasing HDPE content. Moreover, the elongation at break and the impact strength of some HDPE-rich blends exceeded those of pure HDPE polymers.

This work investigated the toughening and deformation mechanisms of PS/HDPE blends compatibilized with SEBS by means of tensile dilatometry. Moreover, we attempt to use the essential work of fracture concept to determine the fracture toughness of the PS/HDPE/SEBS 10/80/10 blend. This blend is selected because its tensile ductility is much higher than that of pure HDPE.[3] The essential work method was originally developed by Broberg[30] for determining the fracture toughness of metallic sheets under plane stress conditions. More recently, several groups used this approach to determine the fracture toughness of ductile polymers.[31–33]

EXPERIMENTAL

Materials

The homopolymers used in this investigation were commercial grades of PS (Styron 667, Dow Chemical Company) and HDPE (blow film B5429, Mobil, Saudi Arabia). The triblock SEBS copolymer (G1652) was kindly supplied by Shell Company with the respective molecular weights of the PS block and central EB block being 7500 and 37,500, respectively, and the PS weight fraction being 28.6%.

Blending Prodedures

All materials used were dried overnight separately in ovens operated at 80°C for PS and HDPE and at 60°C for SEBS. The HDPE/PS blends were prepared by mixing the well-dried pellets in a twin-screw extruder (Brabender Plasticorder) operated at 190–200°C. The compositions of HDPE/PS blends prepared were 70/20, 50/40, 30/60, 20/70, and 10/80 (by weight) and 10 wt % SEBS was added as a compatibilizer.

The extrudates exiting from the extruder were pelletized and then dried at 100°C for 12 h. Using these pellets, dogbone-shaped tensile bars (ASTM D638-91, type I) were injection molded using a Chen Hsong machine. The barrel zone temperatures were set at 200, 210, and 220°C. Furthermore, plaques with dimensions of 200 × 80 × 3.2 mm were also injection molded. For the purpose of comparison, pure PS and HDPE samples were also injection molded under similar processing conditions.

Mechanical Measurements

The tensile experiments were conducted at room temperature (22°C) using an Instron tensile tester (model 4206) at a crosshead speed of 10 mm/min. In the tests two extensometers were used to measure the longitudinal and transverse strain simultaneously. To avoid damage to the extensometers during tensile tests, the experiments were interrupted prior to the final failure of specimens.

For essential work measurements, double edge notched tensile specimens with dimensions of 200 × 25 × 3.2 mm were used. They were cut from the injection molded plaques with the longitudinal direction of the specimens parallel to the melt flow direction. The notch was made by saw cutting a slot, followed by sharpening with a fresh

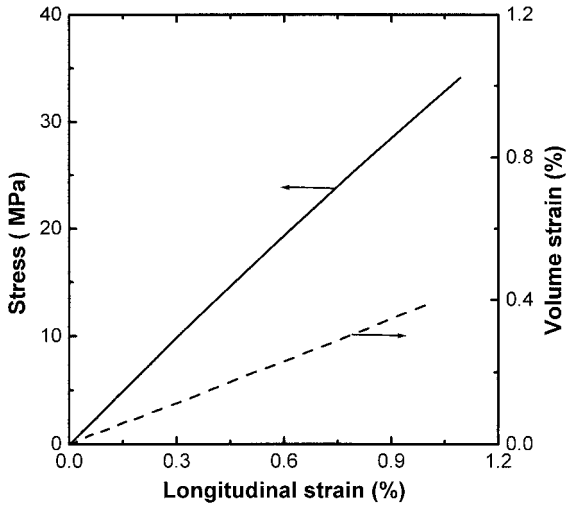

Figure 1 Plots of engineering stress and volume strain versus longitudinal strain for pure PS.

razor blade. The exact ligament length (L) was measured by a traveling microscope (Topcon Profile Projector). The load applied during extension was monitored with a load cell of an Instron tensile tester (model 4206) under a crosshead speed of 10 mm/min.

RESULTS AND DISCUSSION

According to the literature,[18,34–37] the volume strain of specimens during creep or tensile deformation can be determined from the following equation:

$$\frac{\Delta V}{V} = (1 + \varepsilon_l)(1 + \varepsilon_w)(1 + \varepsilon_t) - 1 \qquad (1)$$

where ΔV is the change in volume; V is the original volume; the ratio V/V is the volume strain; and ϵ_l, ϵ_w, and ϵ_t are the longitudinal, transverse, and thickness engineering strains, respectively. Generally, the thickness strain is assumed to be the same as the transverse strain.[38] Therefore, eq. (1) can be simplified as

$$\frac{\Delta V}{V} = (1 + \varepsilon_l)(1 + \varepsilon_t)^2 - 1 \qquad (2)$$

Figure 1 shows the engineering stress and volume strain versus longitudinal strain curves for PS. Apparently, pure PS exhibits a typical characteristic of brittle polymers (i.e., absence of yielding and necking prior to final fracture). In the range of strains studied, the volume strain for pure PS increases linearly with the longitudinal strain. On the contrary, HDPE exhibits ductile behavior during extension. The engineering stress and volume change versus the elongation strain curve for HDPE are shown in Figure 2. Necking was observed during the tensile deformation process. As the neck propagates through the entire gauge length of the specimen, the ultimate elongation can reach about 380%.[3] Although HDPE can undergo extensive plastic deformation prior to final fracture, the volume change of the sample during the tensile process is very small.

Figure 3(a,b) shows the engineering stress and volume strain versus the longitudinal strain curves for the SEBS compatibilized PS/HDPE blends. A dramatic improvement in PS ductility is observed with the incorporation of 20 wt % HDPE to the PS [Fig. 3(a)]. The tensile behavior of this blend is characterized by the occurrence of yielding and necking, followed by homogeneous drawing. This is the typical characteristic of toughened plastics such as HIPS. Similar tensile behavior is observed for the PS/HDPE 50/40 blend [Fig. 3(b)]. However, the yield point becomes less obvious with increasing HDPE content to 60 wt % and above [Fig. 3(c,d)]. It is noted that the volume change of the PS/HDPE/SEBS blends during the tensile process tends to become smaller with increasing the volume content of HDPE in the blends. Moreover, the volume dilation response curves of these blends are not linear, indicating that the deformation mechanisms for these blends are rather complex.

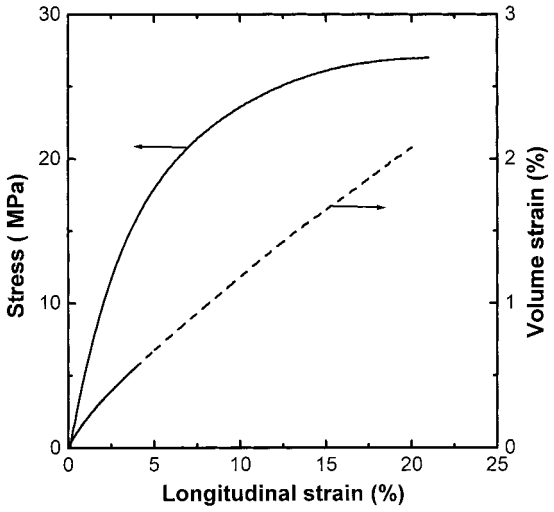

Figure 2 Plots of engineering stress and volume strain versus longitudinal strain for pure HDPE.

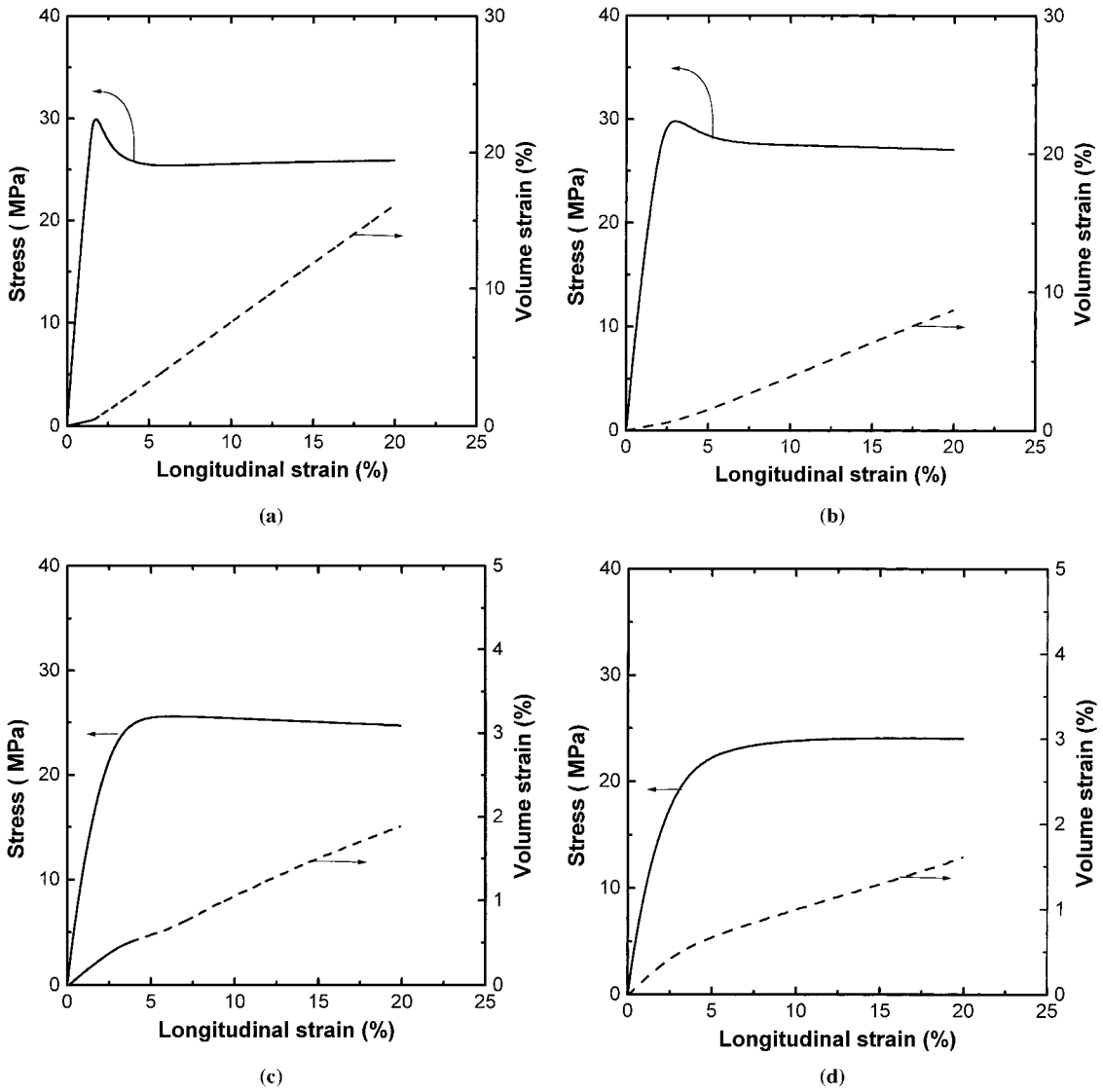

Figure 3 Plots of engineering stress and volume strain versus longitudinal strain for PS/HDPE blends compatibilized by 10 wt % SEBS. (a) PS/HDPE 70/20, (b) PS/HDPE 50/40, (c) PS/HDPE 30/60, and (d) PS/HDPE 10/80.

In order to determine the contributions of various deformations (i.e., elastic, shear, and crazing) to the total elongation, a quantitative model proposed by Heikens et al.[39] was adopted in this study. In that simple model the respective contributions of elastic deformation, shear deformation, and crazing to the total elongation strain and the total volume strain are assumed to be additive, and the amount of material that deforms elastically is considered to remain constant during the entire tensile process. Furthermore, it is assumed that shear deformation makes a negligible contribution to the volume strain and the volume strain caused by crazing is assumed to be equal to the elongation strain. Moreover, crazing is assumed to be the only cavitation mechanism and other cavitation processes are neglected, although debonding at the interface and cavitation of SEBS could also contribute to the volume strain. Another criteria for use of this model is that the specimen must elongate uniformly throughout the entire gauge portion.[13] This implies this model may only be applied to the polymer specimens prior to necking. In this study necking occurs at a strain of about 20% for HDPE. However, the yield point initiates at a lower strain than necking for some blends (e.g., PS/HDPE 70/20 and 50/40) and necking also occurs at about 20%

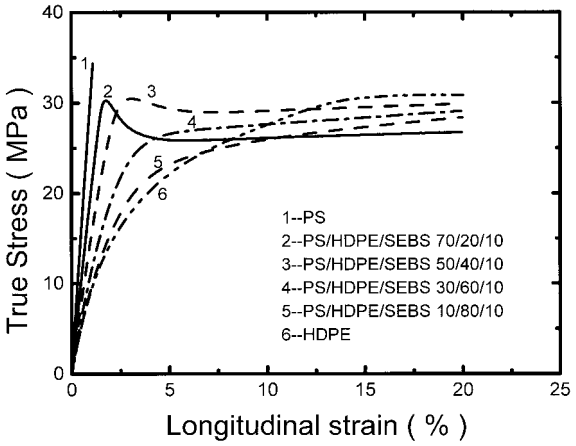

Figure 4 True stress–strain curves for (a) pure PS, (b) PS/HDPE/SEBS 70/20/10, (c) PS/HDPE/SEBS 50/40/10, (d) PS/HDPE/SEBS 30/60/10, (e) PS/HDPE/SEBS 10/80/10, and (f) pure HDPE.

strain. Furthermore, the cross-sectional areas of these blend specimens do not show obvious changes prior to necking. Therefore, we can explore the deformation mechanisms up to an elongation strain of 20% for HDPE and its blends. According to this model, at any elongation strain the strains caused by elastic deformation (ϵ_{el}), shear deformation (ϵ_{sh}), and crazing (ϵ_{cr}) can be calculated from σ_T–ϵ–$\Delta V/V$ diagrams and are given by the following equations[13]:

$$\varepsilon_{el} = \frac{\sigma_T}{E} \tag{3}$$

$$\varepsilon_{cr} = \frac{\Delta V}{V} - \frac{(1-2\nu)\sigma_T}{E} \tag{4}$$

$$\varepsilon_{sh} = \varepsilon - \frac{\Delta V}{V} - \frac{2\nu\sigma_T}{E} \tag{5}$$

where σ_T is the true stress, E is Young's modulus, ϵ is the elongation strain, and ν is the Poisson's ratio. The E and ν can be determined from the initial slopes of $\sigma_{eng} - \epsilon$ (σ_{eng} is the engineering stress) and ϵ_t–ϵ curves, respectively. The true stress is calculated using the instantaneous cross-sectional area over which the deformation occurs. The relation between the true and engineering stresses is

$$\sigma_T = \frac{\sigma_{eng}}{(1+\varepsilon_t)^2} \tag{6}$$

The curves showing the true stress versus the elongation strain for PS, HDPE, and their blends are displayed in Figure 4.

The elongation strains caused by the elastic deformation, shear deformation, and crazing as a function of the total longitudinal strain for PS are shown in Figure 5. It can be seen that elastic deformation is the dominant deformation mechanism over the whole strain range studied. The deformations produced by crazing and shearing are minute relative to the elastic deformation. It is also noted that the critical strain to initiate crazes is smaller than that required to induce shear deformation for PS. It is well known that the plastic deformation of glassy polymers may advance either by shearing or crazing,[40] depending mainly on the critical strain (or stress) that is required to initiate it. In PS the crazing generally occurs at lower applied stress than shearing. Thus, crazing is the main plastic deformation mode of PS during the tensile process.

Figure 6(a) shows the separate contributions of the elastic deformation, shear deformation, and crazing during the tensile deformation for the PS/HDPE/SEBS 70/20/10 blend. As mentioned above, the elastic deformation strain is determined from the true stress divided by the Young's modulus. Therefore, the variation of the elastic deformation with the longitudinal strain shows a variation trend similar to the true stress versus strain curve. An abrupt decrease in elastic deformation in Figure 6(a) corresponds to the yield point in the plot of the true stress versus strain

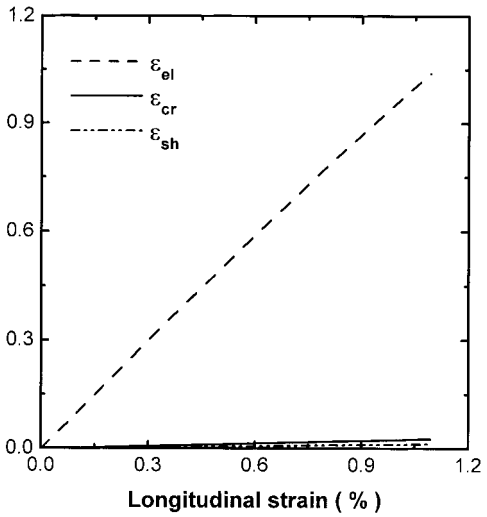

Figure 5 Plots of the elongation strains caused by elastic deformation, shear deformation, and crazing versus the total elongation strain for pure PS.

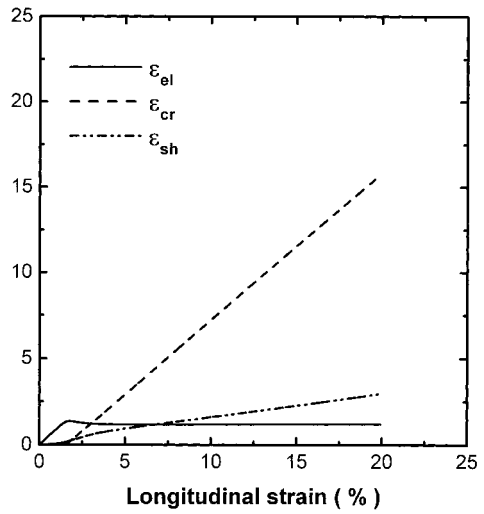

(a)

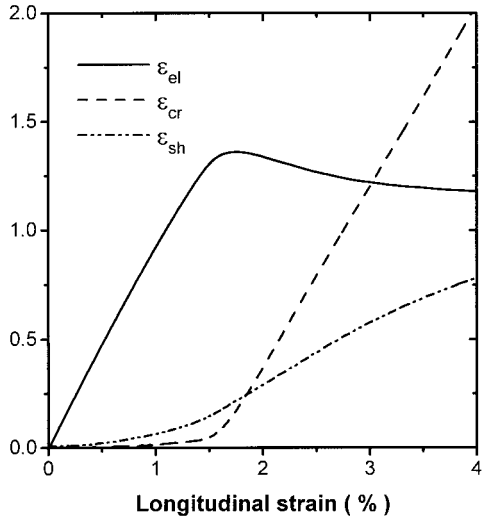

(b)

Figure 6 Plots of the elongation strains caused by elastic deformation, shear deformation, and crazing versus the total elongation strain for the PS/HDPE/SEBS 70/20/10 blend (a) at the whole strain range and (b) up to a strain of 4%.

curve. It can also be seen from Figure 6(a) that the elastic deformation is the main deformation mode prior to yielding. Thereafter plastic deformation portions (including crazing and shearing) increase, and they eventually become the dominant deformation mode. In order to analyze the deformation mechanism prior to yielding, the onset of longitudinal strain is enlarged as shown in Figure 6(b). It is apparent from this figure that the shear deformation is the dominant plastic deformation mechanism at a low elongation strain (less than 1.8%). As the strain exceeds 1.8%, crazing deformation predominates over shearing. In our previous study SEM observation revealed that the HDPE particles are homogeneously dispersed in the PS matrix of the PS/HDPE/SEBS 70/20/10 blend, and the dispersed particles strongly adhere to the matrix (Fig. 7). The mechanical measurements indicated that this blend also exhibits excellent tensile ductility and impact toughness.[3] From the dilatometric analysis it is apparent that the toughening mechanism of the blend is mainly caused by crazing. During tensile deformation, the crazes were first initiated at the periphery of these spherical HDPE particles. The applied stresses were then transferred from the matrix to the dispersed HDPE particles because of a strong interfacial adhesion whereas the dispersed HDPE particles were deformed by shear. Therefore, these two kinds of plastic deformation occurred simultaneously and competed with each other during the tensile process of the PS/HDPE/SEBS 70/20/10 [Fig. 6(a)].

Figure 8 shows the plots of elongation strains due to elastic deformation, shear deformation, and crazing versus the total elongation strain for the PS/HDPE/SEBS 50/40/10. Similarly, elastic deformation is still the main deformation mode prior to yielding. Thereafter plastic deformation is the predominant mode. Crazing initiates at a relatively higher strain, and shear deformation is the dominant plastic deformation mechanism for the whole range of strains. The PS/HDPE/SEBS 50/40/10 blend exhibits a bicontinuous two-phase structure (Fig. 9). Because the critical stress to

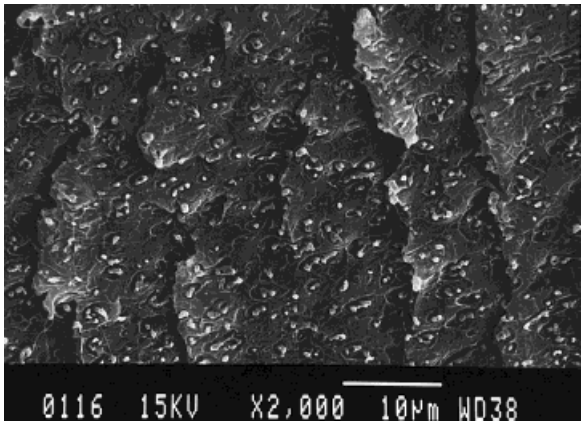

Figure 7 An SEM micrograph showing the cryogenically fractured surface of a PS/HDPE/SEBS 70/20/10 blend.[3]

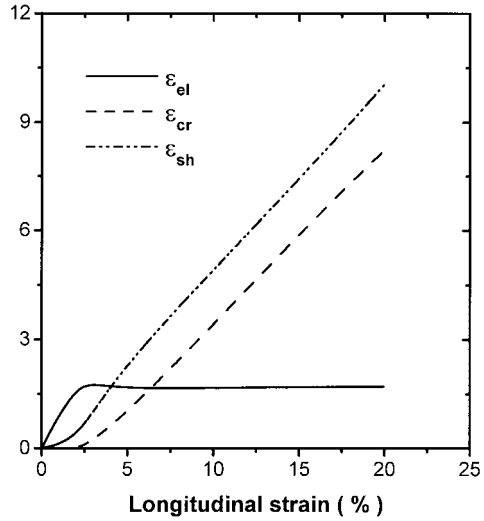

Figure 8 Plots of the elongation strains caused by elastic deformation, shear deformation, and crazing versus the total elongation strain for the PS/HDPE/SEBS 50/40/10 blend.

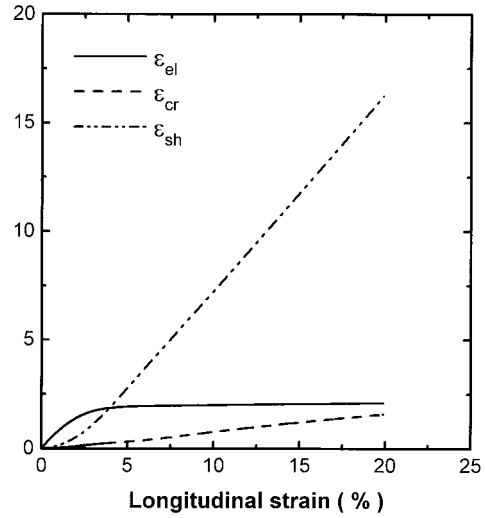

Figure 10 Plots of the elongation strains caused by elastic deformation, shear deformation, and crazing versus the total elongation strain for the PS/HDPE/SEBS 30/60/10 blend.

initiate shearing of HDPE is lower than that required to initiate crazes in PS, the shearing of the HDPE phase occurs at a lower strain but crazing of the PS phase occurs at a higher strain.

As the content of HDPE is increased to 60 wt % (PS/HDPE/SEBS 30/60/10), the shear deformation tends to predominate over crazing (Fig. 10). Moreover, the crazing deformation is smaller than the elastic deformation in the whole range of strain studied. A similar tensile deformation is observed for the PS/HDPE/SEBS 10/80/10 blend (Fig. 11). Finally, Figure 12 shows the tensile dilatometric behavior of pure HDPE: it is obvious that shear deformation predominates.

As mentioned above, the PS/HDPE/SEBS 10/80/10 blend exhibits excellent tensile ductility and impact toughness. Thus, the fracture toughness of this ductile polymer blend can be evaluated by means of the essential work concept. The concept divides the total work of fracture (W_f) into two parts: the essential work of fracture (W_e) re-

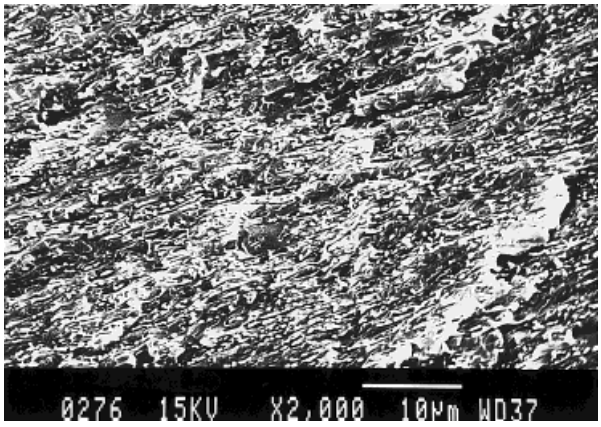

Figure 9 An SEM micrograph showing the cryogenically fractured surface of a PS/HDPE/SEBS 50/40/10 blend.[3]

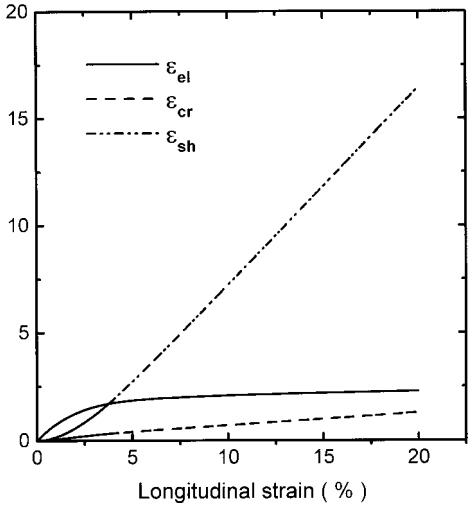

Figure 11 Plots of the elongation strains caused by elastic deformation, shear deformation, and crazing versus the total elongation strain for the PS/HDPE/SEBS 10/80/10 blend.

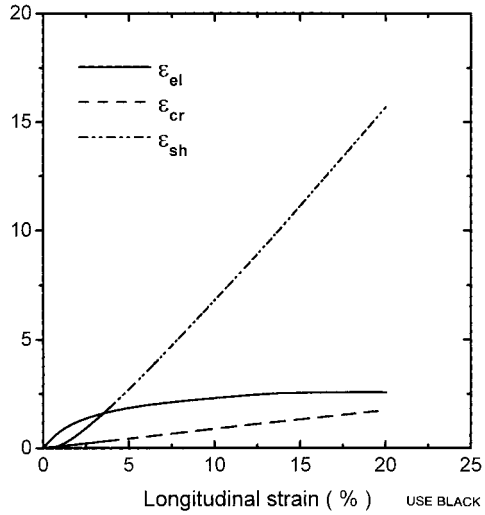

Figure 12 Plots of the elongation strains caused by elastic deformation, shear deformation, and crazing versus the total elongation strain for pure HDPE.

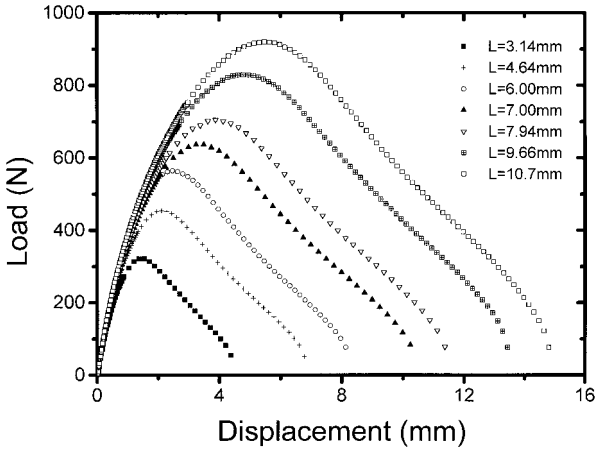

Figure 13 Load–displacement diagrams for double edge notched tensile specimens of a PS/HDPE/SEBS 10/80/10 blend at various ligament lengths tested at a crosshead displacement rate of 10 mm/min (sample width = 25 mm, gauge length = 100 mm).

quired to fracture the polymer in its process zone and nonessential or plastic work (W_p) consumed by various deformation mechanisms in the plastic zone.[30] Therefore, W_f can be expresssed as

$$W_f = W_e + W_p \tag{7}$$

Taking into consideration that *We* is surface related whereas W_p is volume related, W_f can be given by the related specific work terms (i.e., w_e and w_p, respectively)[32]

$$W_f = w_e L t + \beta w_p L^2 t \tag{8}$$

$$w_f = \frac{W_f}{Lt} = w_e + \beta w_p L \tag{9}$$

where L is the ligament length, t is the thickness of the specimen, and β is a shape factor related to the form of the plastic zone. Based on eq. (9), the specific essential work can be easily obtained from the intercept of the linear plot of w_f versus L. However, the explicit determination of w_p is very difficult because of the lack of knowledge of the shape factor β.

Figure 13 shows the typical load–displacement diagrams of a PS/HDPE/SEBS 10/80/10 blend at various ligament lengths. It is apparent that the blend specimens fracture in a ductile manner under the testing conditions employed here. All specimens exhibit gross yielding and necking in the tensile process. A similarity in the shape of these curves indicates that the fracture mode is independent of ligament length.[33]

Figure 14 shows the variation of w_f with L for the PS/HDPE/SEBS 10/80/10 blend. It is obvious that w_f varies linearly with L for the entire ligament range studied. By extrapolating the straight lines to zero ligament length (Fig. 14), the specific essential work of fracture value can be determined, which is 28.18 kJ/m^2. Finally, the nonessential or plastic work term (βw_p), which is determined from the slope of the w_e versus ligament lines, is 19.92 kJ/m^2.

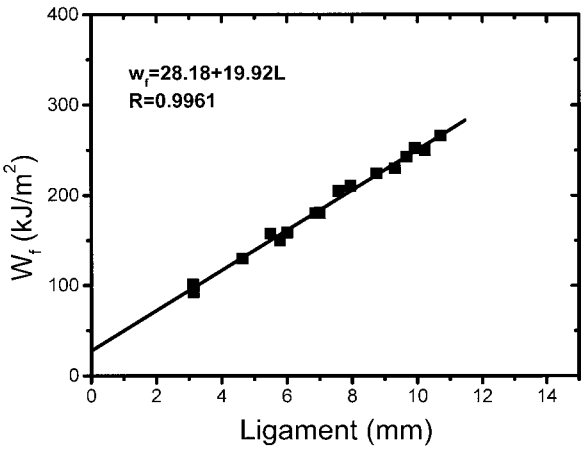

Figure 14 The total specific work of fracture (w_f) vs. ligament length (L) for a PS/HDPE/SEBS 10/80/10 blend at a crosshead displacement rate of 10 mm/min (sample width = 25 mm, gauge length = 100 mm).

From the above results it is apparent that the volume dilatometric method can be used to describe the deformation mechanisms of brittle PS and ductile PS/HDPE/SEBS polymer blends under an applied uniaxial load. In the ductile polymer blends the relative contributions of the craze and shear yielding can be determined effectively. Therefore, we can discern which deformation mechanism prevails in ductile polymers during static loading. Generally, the toughening behavior of ductile polymer blends can be determined by means of the *J*-integral approach.[41,42] According to ASTM standards, the critical *J* integral (J_{IC}) should be determined by the intersection of a crack growth resistance curve and a crack blunting line.[43–45] However, the blunting line approach was questioned with regard to its ability to determine the critical *J*-integral value for crack initiation of elastomer toughened polymers.[46] It should be noted that the volume dilatometric and *J*-integral approaches can yield satisfactory results under a quasistatic state of loading. For the dilatometric approach, it is expected that the contribution of shear yielding of ductile polymers to the total deformation becomes smaller under a high rate of loading. Finally, the toughening behavior of ductile polymers under a high rate of loading is generally examined by impact tests. The impact behavior of PS/HDPE/SEBS blends was investigated in a previous study.[3]

CONCLUSIONS

1. A simple quantitative model developed by Heikens et al.[39] can be used to analyze the tensile deformation mechanisms of SEBS compatibilized PS/HDPE blends. The separate contributions of elastic deformation, shear deformation, and crazing to the total elongation can be determined.
2. For a brittle PS polymer the critical strain required to start crazing is considerably lower than that required to induce shear deformation. Therefore, crazing is the main nonelastic deformation mode of PS in a tensile process. On the contrary, shear deformation is the main plastic mode during the tensile process of HDPE.
3. For all of the SEBS compatibilized PS/HDPE blends, the elastic deformation is the dominant deformation mechanism prior to yielding; thereafter the plastic deformations (including shearing and crazing) predominate.
4. Crazing is the main plastic deformation mode after yielding for the PS/HDPE/SEBS 70/20/10 blend. The toughening mechanism of the blend is crazing rather than shearing. However, the shear deformation gradually becomes the predominant plastic deformation mode as the content of HDPE is increased.
5. The essential work and nonessential work term of the PS/HDPE/SEBS 70/20/10 blend were determined to be 28.18 and 19.92 kJ/m^2, respectively.

S.A.X. would like to thank the Croucher Foundation for providing a fellowship to visit the City University of Hong Kong.

REFERENCES

1. Kramer, E. J. Adv Polym Sci 1983, 52/53, 1.
2. Argon, A. S.; Cohen, R. E. Adv Polym Sci 1990, 91/92, 1.
3. Tjong, S. C.; Xu, S. A. J Appl Polym Sci 1998, 68, 1099.
4. Linsey, C. R.; Paul, D. R.; Barlow, J. W. J Appl Polym Sci 1981, 26, 1.
5. Fayt, R.; Jerome, R.; Teyssie, P. J Polym Sci Polym Phys Ed 1989, 27, 775.
6. Mekhilef, N.; Favis, B. D.; Carreau, P. J. J Polym Sci Polym Phys Ed 1997, 35, 293.
7. Xu, S. A.; Jiang, M.; Shen, J. S. Polym J 1996, 28, 226.
8. Xu, S. A.; Chan, C. M. Polym J 1998, 30, 552.
9. Fayt, R.; Jerome, R.; Teyssie, P. J Polym Sci Polym Phys Ed 1982, 20, 2209.
10. Coumans, W. J.; Heikens, D. Polymer 1981, 21, 957.
11. Coumans, W. J.; Heikens, D.; Sjoerdsma, S. D. Polymer 1981, 21, 103.
12. Dekkers, M. E. J.; Heikens, D. J Appl Polym Sci 1983, 28, 3809.
13. Dekkers, M. E. J.; Heikens, D. J Appl Polym Sci 1985, 30, 2389.
14. Dekkers, M. E. J.; Heikens, D. J Mater Sci 1985, 20, 3873.
15. Dekkers, M. E. J.; Hobbs, S. Y.; Watkins, V. H. J Mater Sci 1988, 23, 1225.
16. Hobbs, S. Y.; Dekkers, M. E. J. J Mater Sci 1989, 24, 1316.
17. Bucknall, C. B.; Clayton, D.; Keast, W. J Mater Sci 1972, 7, 1443.

18. Bucknall, C. B.; Clayton, D.; Keast, W. J Mater Sci 1973, 8, 514.
19. Bucknall, C. B.; Drinkwater, I. C. J Mater Sci 1972, 8, 1800.
20. Bucknall, C. B.; Stevens, W. W. J Mater Sci 1980, 15, 2950.
21. Bucknall, C. B.; Page, C. J. J Mater Sci 1982, 17, 808.
22. Bucknall, C. B.; Clayton, D.; Keast, W. J Mater Sci 1984, 19, 2064.
23. Bucknall, C. B.; Davies, P.; Partridge, I. K. J Mater Sci 1986, 21, 307.
24. Bucknall, C. B.; Heather, P. S.; Lazzeri, A. J Mater Sci 1989, 24, 2255.
25. Hutchinson, J. M.; Bucknall, C. B. Polym Eng Sci 1980, 20, 173.
26. Naqui, S. I.; Robinson, I. M. J Mater Sci 1993, 28, 1421.
27. Schwarz, J. M. C.; Keskkula, H.; Barlow, J. W.; Paul, D. R. J Appl Polym Sci 1988, 35, 653.
28. Bucknall, C. B.; Clayton, D. J Mater Sci 1972, 7, 202.
29. Bucknall, C. B.; Clayton, D. Nature 1971, 231, 107.
30. Broberg, K. B. Int J Fracture Mech 1968, 4, 11.
31. Hashemi, S. Polym Eng Sci 1997, 37, 912.
32. Kocsis, J. K.; Czigany, T. Polymer 1996, 37, 2433.
33. Kocsis, J. K.; Czigany, T. Polymer 1996, 38, 4587.
34. Truss, R. W.; Chadwick, G. A. J Mater Sci 1976, 11, 111.
35. Truss, R. W.; Chadwick, G. A. J Mater Sci 1976, 11, 1385.
36. Cessna, L. C. Polym Eng Sci 1974, 14, 696.
37. Coumans, W. J.; Heikens, D. Polymer 1980, 21, 957.
38. Nagui, S. I.; Robinson, I. B. J Mater Sci 1993, 28, 1421.
39. Heikens, D.; Sjoerdsma, S. D.; Counians, W. J. J Mater Sci 1973, 8, 514.
40. Bucknall, C. B. Toughened Plastics; Applied Science Publishers: London, 1977.
41. Tjong, S. C.; Ke, Y. C. Polym Eng Sci 1996, 36, 2626.
42. Tjong, S. C.; Ke, Y. C. Eur Polym J 1998, 34, 1565.
43. ASTM Standard E813–81, Annual Book of ASTM Standards; American Society for Testing and Materials: Philadelphia, PA, 1981; Part 10, p 810.
44. ASTM Standard E813–87, Annual Book of ASTM Standards; American Society for Testing and Materials: Philadelphia, PA, 1987; Part 10, p 968.
45. ASTM Standard E813–89, Annual Book of ASTM Standards; American Society for Testing and Materials: Philadelphia, PA, 1989; Part 10, p 628.
46. Narisawa, I.; Takemori, M. T. Polym Eng Sci 1989, 29, 671.